PAMM

WILEY-VCH

SPECIAL ISSUE 94th Annual Meeting of the International Association of Applied Mathematics and Mechanics (GAMM)

RESEARCH ARTICLE OPEN ACCESS

Shape Sensitivity Analysis of History-Dependent Materials for Dynamic Structures

Seyed Ali Ghasemi | Franz-Joseph Barthold

Institute of Structural Mechanics and Dynamics, TU Dortmund University, Dortmund, Germany

Correspondence: Seyed Ali Ghasemi (ali.ghasemi@tu-dortmund.de)

Received: 27 May 2024 | **Revised:** 9 October 2024 | **Accepted:** 19 November 2024

ABSTRACT

This work presents a sensitivity analysis of inelastic material behavior within dynamic structures. The primary focus is on using the direct differentiation method to derive sensitivity matrices for displacement, velocity, acceleration, and history variables. These methods are validated through a detailed academic example.

1 | Introduction

Efficient and lightweight production in design processes relies on structural optimization, where sensitivity analysis plays a crucial role. This study focuses on analytical sensitivity analysis for time-dependent structural behavior. Specifically, the design sensitivity formulations for the direct differentiation method (DDM). In structural optimization, DDM computes sensitivities by directly differentiating the structural response equations concerning design variables. However, it requires solving additional equations for each design variable, resulting in computational expenses, especially for large-scale problems. Despite this drawback, DDM's straightforward implementation suits problems with relatively few design variables. The utilization of isogeometric analysis (IGA) [3] in structural optimization eliminates costly remeshing and design velocity field calculations. IGA's precise geometry description with fewer control points, high-order continuity, and increased flexibility due to control point weights present advantages over conventional finite element method (FEM) approaches. These properties significantly impact shape sensitivity analysis.

2 | Inelastic Structural Dynamic Analysis

The method for solving the general nonlinear motion equation $R = R^{ext} - R^{int} = 0$, with the implicit Newmark method [6] for time discretization and isogeometric asnalysis for spatial discretization, is explored in [1] and [4]. This work employs a nonlinear elastoplastic material model, as described in [7]. The model utilizes the multiplicative decomposition of the deformation gradient $\mathbf{F}$ into elastic $\mathbf{F}^{\mathrm{e}}$ and plastic $\mathbf{F}^{\mathrm{p}}$ parts, alongside the J_2 plasticity formulation. The strain energy function for the elastoplastic material model is expressed as follows:

$$W = \frac{1}{2}K\left[\frac{1}{2}\left(J_e{}^2 - 1\right) - \ln J_e + \frac{1}{2}G\left(\operatorname{tr}\widetilde{C}_e - 3\right)\right]. \tag{1}$$

Here, K, G, J_e, and $\widetilde{C}_e$ represent the compression modulus, shear modulus, determinant of the elastic deformation gradient, and the elastic isochoric right Cauchy–Green tensor, respectively. The stress calculation utilizes the radial return-mapping algorithm, as depicted in 1, employing a two-step approach to determine local stress. Initially, the deformation state is assumed purely elastic, and the elastic trial state is computed within the elastic predictor step. To compute the trial state, the variables $\widetilde{C}_p^{-1}$ and α from the previous time step are required. Thus, a history field $\boldsymbol{h} = \{\widetilde{C}_p^{-1}, \alpha\}$ is necessary. At time t_0, the history field is initialized and saved at the end of a converged time step within the Newton–Raphson method. When the yielding condition is met, there is no evolution in the history variables. Conversely, if the trial state violates the yielding condition, the history field needs updating. The Von Mises yield function is defined as a function of the deviatoric part of the Kirchhoff stress tensor as $\phi = ||\mathbf{s}^{tr}|| - \sqrt{\frac{2}{3}}\kappa(\alpha)$. Here,

ALGORITHM 1 | Return-mapping algorithm for J_2-plasticity.

Input: $\mathbf{F}$: deformation gradient, K: compression modulus, G: shear modulus, $\mathbf{h}_n$: history variables

procedure 1 - Load history variables
  $\boldsymbol{h}_n = \{\widetilde{\mathbf{C}}_p^{-1}, \alpha\}$
end procedure
procedure 2 - Calculate elastic predictor
  $\widetilde{\mathbf{F}} = J^{-\frac{1}{3}}\,\mathbf{F},$
  $\widetilde{b}_e^{tr} = \widetilde{\mathbf{F}}\widetilde{C}_p^{-1}\widetilde{\mathbf{F}}^T$
  $\mathbf{s}^{tr} = G\,\mathrm{dev}\,\widetilde{b}_e^{tr}, \quad \mathbf{s}^{tr} = \mathrm{dev}\,\tau^{tr}$
  $\mu = \frac{1}{3}G\,\mathrm{tr}\,\widetilde{b}_e^{tr}$
end procedure
procedure 3 - Check for plastic loading
  if $\phi^{tr} = ||\mathbf{s}^{tr}|| - \sqrt{\frac{2}{3}}\kappa(\alpha_n) \leq 0$ **then** elastic state $\rightarrow$ update(.) = $(.)^{tr}$
  else plastic corrector
    calculate $\Delta\gamma$ using local Newton-Raphson algorithm
    $\mathbf{n} = \frac{\mathbf{s}^{tr}}{||\mathbf{s}^{tr}||}$
    $\mathbf{s} = \mathbf{s}^{tr} - 2\mu\,\Delta\gamma\mathbf{n}$
    $\alpha = \alpha_n + \sqrt{\frac{2}{3}}\Delta\gamma,$
    $\mathbf{s} = \frac{1}{G}(\mathbf{s} + \mu\mathbf{I})$
    $\widetilde{C}_p^{-1} = \widetilde{\mathbf{F}}^{-1}\widetilde{b}_e^{tr}\widetilde{\mathbf{F}}^{-T}$
  end if
end procedure
procedure 4 - Stress update
  $\mathbf{P} = [\frac{1}{2}KJ(J^2-1)\mathbf{I} + \mathbf{s}]\mathbf{F}^{-T}$
end procedure
procedure 5 - Material tensor
  $\mathbb{A} = \frac{\partial \mathbf{P}}{\partial \mathbf{F}}$
end procedure
procedure 6 - Save history variables
  $\mathbf{h}_{n+1} = \{\widetilde{\mathbf{C}}_p^{-1}, \alpha\}$
end procedure

Output: $\mathbf{P}$: stress, $\mathbb{A}$: material tensor, $\mathbf{h}_{n+1}$: history variables

$\mathbf{s}^{tr}$ represents the deviatoric trial stress tensor and the nonlinear hardening κ is a function of the hardening variable α and it is defined as follows: $\kappa(\alpha) = \sigma_0 + \sigma_\infty\,(1 - \exp(-d\,\alpha)) + H\alpha$, where H is the linear hardening, and d is a dimensionless parameter. The initial yield stress σ_0 and limit yield stress σ_∞ are material properties. The time derivative of the hardening variable α is given by $\frac{d\alpha}{dt} = \sqrt{\frac{2}{3}}\frac{d\gamma}{dt}$, where γ is the plastic multiplier. Employing the local Newton–Raphson method detailed in Algorithm 2, the plastic multiplier increment $\Delta\gamma$ must be computed from $\phi(\Delta\gamma) = ||\mathbf{s}^{tr}|| - \sqrt{\frac{2}{3}}\kappa(\alpha + \sqrt{\frac{2}{3}}\Delta\gamma) - 2\mu\Delta\gamma = 0$. Here, μ is defined as $\mu = \frac{1}{3}G\,\mathrm{tr}\,\widetilde{\mathbf{b}}_e^{tr}$.

ALGORITHM 2 | Local Newton–Raphson.

1: start value $\Delta\gamma = 0$
2: **while** $\phi(\Delta\gamma^i) > 0$ **do**
3: $\quad\phi(\Delta\gamma^i) = ||\mathbf{s}^{tr}|| - \sqrt{\frac{2}{3}}\kappa(\Delta\gamma^i) - 2\mu\Delta\gamma^i$
4: $\quad\phi'(\Delta\gamma^i) = -2\mu - \frac{2}{3}\kappa'(\Delta\gamma^i)$
5: $\quad\Delta\gamma^{i+1} = \Delta\gamma^i - \frac{\phi(\Delta\gamma^i)}{\phi'(\Delta\gamma^i)}$
6: **end while**

Figure 1 demonstrates the structural analysis of inelastic material behavior using the implicit Newmark method. Following the setup in the pre-processing stage, time parameters and step size must be specified or determined. Subsequently, if the current time is not the final time, structural analysis is conducted

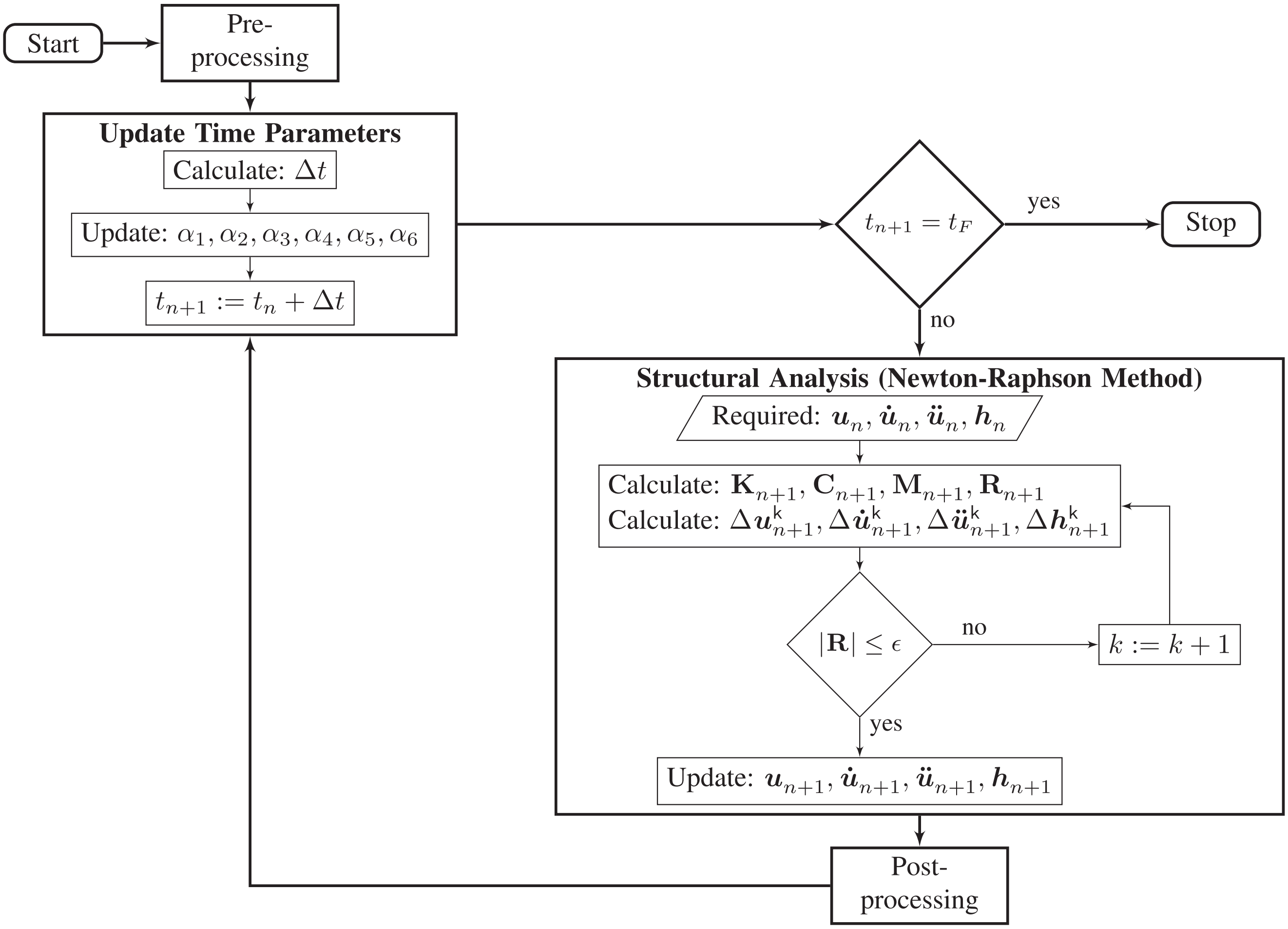

FIGURE 1 | Structural analysis algorithm.

employing the Newton–Raphson method. Within this stage, state and history variables from previous time steps are necessary. At each Newton–Raphson iteration, the total residual is computed, and convergence of the current solution is checked. If convergence has not been reached, the algorithm proceeds to the next Newton–Raphson iteration. Upon convergence, it proceeds to the post-processing step and then moves to the next time step until reaching the final time.

3 | Sensitivity Analysis

In this section, various differentiation techniques are briefly discussed. Then, the direct method is utilized to obtain dynamic response sensitivities for inelastic materials.

3.1 | Differentiation Techniques

Within sensitivity analysis, computing derivatives plays an important role. Figure 2 shows various differentiation techniques. These techniques are divided into the following three main categories: numerical methods, analytical methods, and semi-analytical methods. Finite difference methods (FDMs) and the complex step method (CSM) are numerical methods that compute approximations of derivatives by evaluating function values. Both approaches are derived from a Taylor series expansion. The three schemes of finite difference methods are forward (FFD), backward (BFD), and central (CFD). The forward difference scheme derives the function's derivative at a point by evaluating function values at the point and the point ahead. Conversely, the backward difference method employs function values at the point and the preceding point in computing the derivative. The central difference method provides better accuracy through function values on both sides of the point of interest. FDMs are widely used due to their simplicity. The accuracy of the approximation depends on the choice of step size. The CSM compared to FDMs uses an imaginary step. This method uses complex arithmetic to calculate the numerical value of the first derivative of a real function. CSM has no subtractive cancellation error and the truncation error can be avoided for a small step size.

Analytical methods are divided into the following three main categories: automatic differentiation (AD), symbolic differentiation, and manual differentiation. Unlike numerical techniques, there are no approximations to calculate derivatives.

AD computes derivatives of functions by applying chain rules. It decomposes complex functions into simple operations for which derivatives are known. The two modes of AD are forward and reverse.

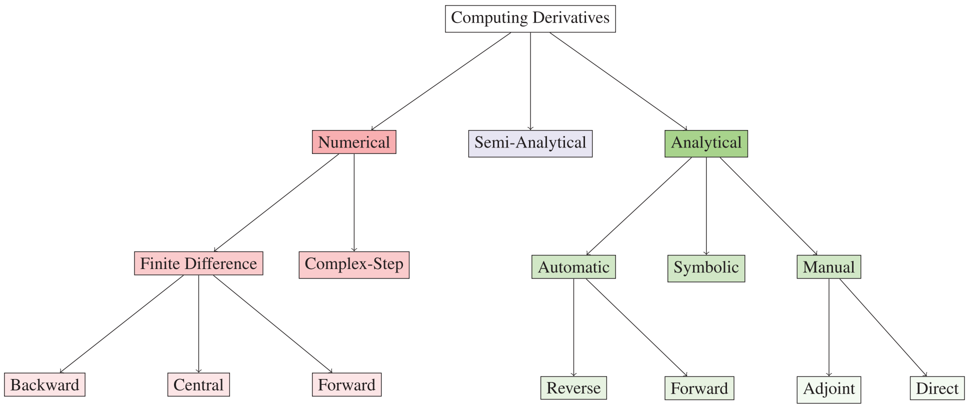

FIGURE 2 | Differentiation techniques.

In symbolic differentiation, derivatives are obtained from symbolic expressions of functions. This technique generates a new mathematical expression for the derivative and can be applied to simple functions. However, for complex functions, this technique is not very useful because it does not simplify the obtained derivatives and leads to lengthy expressions.

Manual differentiation is divided into the following two main categories: the adjoint variable method (AVM) and the direct method. In manual differentiation, derivatives are determined manually, which has the advantage of obtaining simple formulations that can efficiently determine derivatives. Direct differentiation is analogous to the forward mode of AD, while the adjoint method is analogous to the reverse mode. If the number of function evaluations n_f is greater than the number of inputs n_x, it is advantageous to use the direct method because this method requires solving n_x times. Conversely, if the number of inputs n_x is greater than the number of function evaluations n_f, it is advantageous to use the adjoint method because this method requires solving n_f times.

The semi-analytical technique combines analytical methods with numerical methods. This means that if obtaining certain partial derivatives within the direct method or adjoint method is difficult, they can be calculated numerically.

In this work, the DDM is used for sensitivity analysis. Within IGA, the geometry can be described using a smaller number of control points. These control points are the geometrical design variables and as the number of design variables is not large, the direct method is suitable.

3.2 | Inelastic Dynamic Response Sensitivities

Following the determination of a dynamic solution state, design sensitivity analysis is conducted to extract gradient information of the current state concerning selected geometric design variables $\boldsymbol{s}$, see [2, 4]. It is crucial to ensure that any total design variation does not violate the force equilibrium of the dynamic system, as defined in the residual equation

$$\delta\mathbf{R} = \delta\mathbf{R}^{\text{ext}} - \delta\mathbf{R}^{\text{int}} = \mathbf{0}. \tag{2}$$

The response sensitivities for nonlinear dynamics using the implicit Newmark method are discussed in [1]. In this study, the formulations are extended to accommodate history-dependent materials. For detailed information on the sensitivity analysis of inelastic materials for static analysis, refer to [5]. Functional dependencies

$$\mathbf{R} = \mathbf{R}(\ddot{\boldsymbol{u}}_{n+1}, \dot{\boldsymbol{u}}_{n+1}, \boldsymbol{u}_{n+1}, \boldsymbol{h}_{n+1}, \boldsymbol{s})$$

are considered and the variation of the internal part yields the following:

$$\delta\mathbf{R}^{\text{int}} = \mathbf{M}\delta\ddot{\boldsymbol{u}}_{n+1} + \mathbf{C}\delta\dot{\boldsymbol{u}}_{n+1} + \mathbf{K}\delta\boldsymbol{u}_{n+1} + \mathbf{H}\delta\boldsymbol{h}_n + \mathbf{P}^{\text{int}}\delta\boldsymbol{s}, \tag{3}$$

where $\mathbf{M}$, $\mathbf{C}$, and $\mathbf{K}$ represent the mass, damping, and stiffness matrices, respectively. $\mathbf{H} = \frac{\partial\mathbf{R}^{\text{int}}}{\partial\boldsymbol{h}_n}$ is the history sensitivity matrix and $\mathbf{P}^{\text{int}} = \frac{\partial\mathbf{R}^{\text{int}}}{\partial\boldsymbol{s}}$ is the internal pseudo-load matrix.

If the external part is assumed to be independent of the dynamic state and history variables, the variation of the external part of the residual can be expressed as follows:

$$\delta\mathbf{R}^{\text{ext}} = \delta\mathbf{F}^{v} + \delta\mathbf{F}^{s} + \delta\mathbf{F}^{l} + \delta\mathbf{F}^{n} = \mathbf{P}^{\text{ext}}\delta\boldsymbol{s}, \tag{4}$$

where $\mathbf{P}^{\text{ext}}$ is defined as $\mathbf{P}^{\text{ext}} = \frac{\partial\mathbf{R}^{\text{ext}}}{\partial\boldsymbol{s}}$. Rearranging Equation (2) leads to the definition of the total sensitivity matrix $\mathbf{S}_{n+1}$, which connects displacements with geometric design variations in the current time step

$$\delta\boldsymbol{u}_{n+1} = -\mathbf{K}^{-1}[\mathbf{P} + \mathbf{D} + \mathbf{Q}]\delta\boldsymbol{s} = \mathbf{S}_{n+1}\delta\boldsymbol{s}. \tag{5}$$

Here, $\mathbf{P} = \mathbf{P}^{\text{ext}} - \mathbf{P}^{\text{int}}$ represents the total pseudo-load matrix and $\mathbf{Q} = -\mathbf{H}\mathbf{G}_n$ is used, where $\mathbf{G}_n$ denotes the total variation of history variables. In Equation (5), $\mathbf{D}$ is the dynamic pseudo-load matrix, represented as follows:

$$\mathbf{D} = -\left[\mathbf{M}\frac{\partial\ddot{\boldsymbol{u}}_{n+1}}{\partial\ddot{\boldsymbol{u}}_n} + \mathbf{C}\frac{\partial\dot{\boldsymbol{u}}_{n+1}}{\partial\ddot{\boldsymbol{u}}_n}\right]\mathbf{A}_n - \left[\mathbf{M}\frac{\partial\ddot{\boldsymbol{u}}_{n+1}}{\partial\dot{\boldsymbol{u}}_n} + \mathbf{C}\frac{\partial\dot{\boldsymbol{u}}_{n+1}}{\partial\dot{\boldsymbol{u}}_n}\right]\mathbf{V}_n - \left[\mathbf{M}\frac{\partial\ddot{\boldsymbol{u}}_{n+1}}{\partial\boldsymbol{u}_n} + \mathbf{C}\frac{\partial\dot{\boldsymbol{u}}_{n+1}}{\partial\boldsymbol{u}_n}\right]\mathbf{S}_n. \tag{6}$$

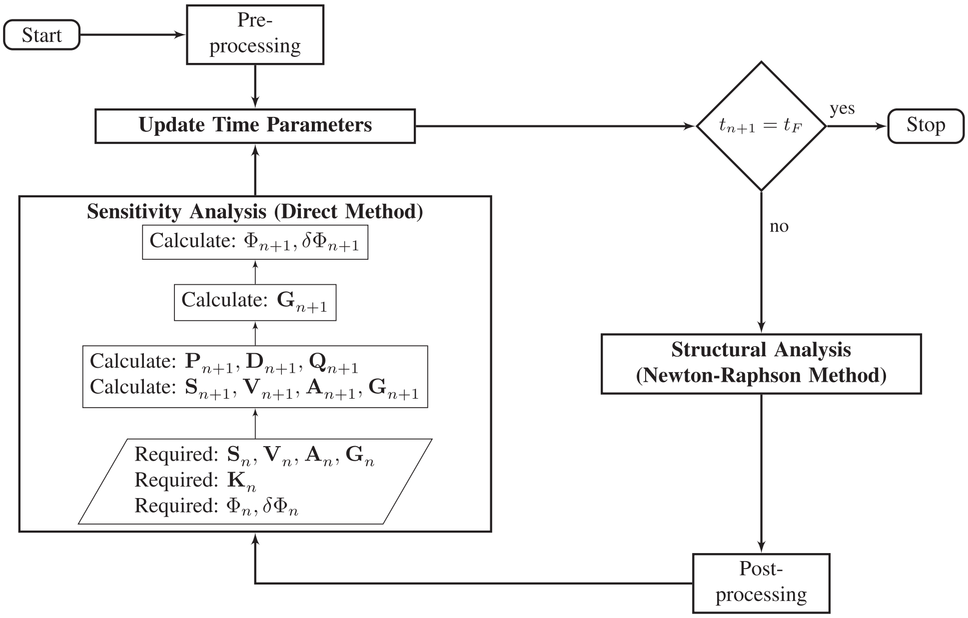

FIGURE 3 | Response sensitivity analysis algorithm.

Here, $\mathbf{V}_n$ and $\mathbf{A}_n$ are velocity and acceleration sensitivity matrices, respectively. At the end of each time step, the dynamic response and history sensitivities are updated as follows:

$$\delta\dot{\boldsymbol{u}}_{n+1} = \left[\frac{\partial\dot{\boldsymbol{u}}_{n+1}}{\partial\ddot{\boldsymbol{u}}_n}\mathbf{A}_n + \frac{\partial\dot{\boldsymbol{u}}_{n+1}}{\partial\dot{\boldsymbol{u}}_n}\mathbf{V}_n + \frac{\partial\dot{\boldsymbol{u}}_{n+1}}{\partial\boldsymbol{u}_n}(\mathbf{S}_{n+1} - \mathbf{S}_n)\right]\delta\boldsymbol{s} = \mathbf{V}_{n+1}\delta\boldsymbol{s}, \tag{7}$$

$$\delta\ddot{\boldsymbol{u}}_{n+1} = \left[\frac{\partial\ddot{\boldsymbol{u}}_{n+1}}{\partial\ddot{\boldsymbol{u}}_n}\mathbf{A}_n + \frac{\partial\ddot{\boldsymbol{u}}_{n+1}}{\partial\dot{\boldsymbol{u}}_n}\mathbf{V}_n + \frac{\partial\ddot{\boldsymbol{u}}_{n+1}}{\partial\boldsymbol{u}_n}(\mathbf{S}_{n+1} - \mathbf{S}_n)\right]\delta\boldsymbol{s} = \mathbf{A}_{n+1}\delta\boldsymbol{s}, \tag{8}$$

$$\delta\boldsymbol{h}_{n+1} = \left[\frac{\partial\boldsymbol{h}_{n+1}}{\partial\boldsymbol{h}_n}\mathbf{G}_n + \frac{\partial\boldsymbol{h}_n}{\partial\boldsymbol{u}_{n+1}}\mathbf{S}_{n+1} + \frac{\partial\boldsymbol{h}_n}{\partial\boldsymbol{s}}\right]\delta\boldsymbol{s} = \mathbf{G}_{n+1}\delta\boldsymbol{s}. \tag{9}$$

Geometric design sensitivity information of any physical quantity of interest $\Phi(\boldsymbol{s})$ can be computed by directly inserting the total variations of the dynamic state in form of the sensitivity matrices $\mathbf{S}_{n+1}$, $\mathbf{V}_{n+1}$, and $\mathbf{A}_{n+1}$ and variation of history variables $\mathbf{G}_n$, which leads to the total variation expressed only in terms of design variations

$$\begin{aligned}\delta\Phi &= \delta_{\ddot{\boldsymbol{u}}_{n+1}}\Phi + \delta_{\dot{\boldsymbol{u}}_{n+1}}\Phi + \delta_{\boldsymbol{u}_{n+1}}\Phi + \delta_{\boldsymbol{h}_{n+1}}\Phi + \delta_{\boldsymbol{s}}\Phi \\ &= \left[\frac{\partial\Phi}{\partial\ddot{\boldsymbol{u}}_{n+1}}\mathbf{A}_{n+1} + \frac{\partial\Phi}{\partial\dot{\boldsymbol{u}}_{n+1}}\mathbf{V}_{n+1} + \frac{\partial\Phi}{\partial\boldsymbol{u}_{n+1}}\mathbf{S}_{n+1}\frac{\partial\Phi}{\partial\boldsymbol{h}_n}\mathbf{G}_n + \frac{\partial\Phi}{\partial\boldsymbol{s}}\right]\delta\boldsymbol{s}.\end{aligned} \tag{10}$$

The algorithm to compute sensitivities is provided in Figure 3. After structural analysis converges to a solution, sensitivity analysis is performed in the subsequent step. In this step, physical quantities Φ_n from the previous time step, their variations $\delta\Phi_n$, sensitivity matrices of dynamic variables $\mathbf{S}_n$, $\mathbf{V}_n$, $\mathbf{A}_n$, and sensitivity of history variables $\mathbf{G}_n$ are required. With this information and the calculation of pseudo-load matrices $\mathbf{P}$, $\mathbf{D}$, and $\mathbf{Q}$, it is possible to update sensitivity matrices. For the initial time step t_0, all sensitivity matrices must be calculated or defined.

4 | Numerical Example

This section illustrates a numerical example of three-dimensional geometry described using Non-Uniform Rational B-Splines (NURBS). The physical dimensions are $1000\,\text{mm} \times 100\,\text{mm} \times 100\,\text{mm}$. A parametric space extending uniformly from 0 to 1 along each axis is created. This space is divided into $n_e = [6, 1, 2]$ elements along the respective axes, resulting in a total of 12 elements, with C^0 continuity set between adjacent elements.

To map the discretized parametric points to physical space within the defined parameter space, $n_c = [7, 2, 3]$ control points are required. These points are evenly spaced, each assigned a weight of one, thus forming a B-spline volume shape.For the structural analysis, IGA is utilized, employing NURBS shape functions for geometry description and analysis. This method ensures the model and its analysis are consistent. Boundary conditions are implemented, with the middle two control points on the left surface fixed in all directions, while two on the opposite side are constrained in the z-direction.

The simulation runs over 10 s with a time step of $\Delta t = 0.025$, resulting in a total of 400 steps. To ensure stability and accuracy throughout the simulation, Newmark parameters for average constant acceleration are configured as $\beta = \frac{1}{4}$ and $\gamma = \frac{1}{2}$.

During the simulation, a line load is applied along the centerline of the x-axis on both the front and back surfaces. This load acts downward along the z-axis, increasing from 0 to $-100\,\text{N}$ over the first 80 steps before being released.

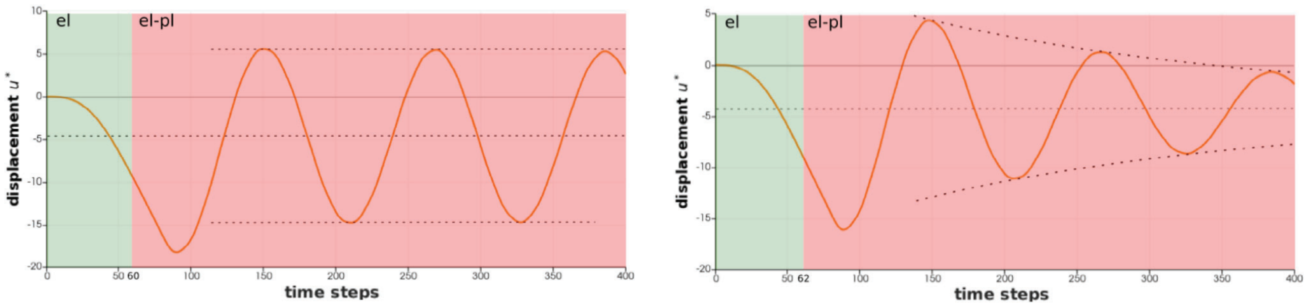

(a) Undamped

(b) Damped

FIGURE 4 | Structural response.

TABLE 1 | Summary of model parameters.

Geometry model	
Basis function	B-splines
Patch dimension	$l_p, w_p, h_p = [0, 1]$
Geometry dimension [mm]	$l = 1000, w = 100, h = 100$
Number of control points	$n_c = [7, 2, 3]$
Analysis model	
Number of elements	12
Degrees of freedom	126
Continuity	C^0
Time parameters	
Time interval [s]	$t = [0, 10]$
Time step	$\Delta t = 0.025$
Newmark parameters	$\beta = \frac{1}{4}, \gamma = \frac{1}{2}$
Material properties	
Elasticity modulus [GPa]	$E = 70$
Poisson's ratio	$\nu = 0.3$
Initial yield stress [GPa]	$\sigma_0 = 0.265$
Hardening	$H = 16.93$
Density $\left[\mathrm{kg}/\,\mathrm{m}^3\,\mathrm{m}\right]$	$\rho = 2.7e^{-6}$
Damping coefficients	$c_1 = \{0,\ 0.3\}, c_2 = 0$

The material properties are set with an elasticity modulus of $E = 70\,\mathrm{GPa}$, a Poisson's ratio of $\nu = 0.3$, and a density of $\rho = 0.265\,\frac{\mathrm{kg}}{\mathrm{m}^3\,\mathrm{m}}$. The initial yield stress is $\sigma_0 = 0.265\,\mathrm{GPa}$ with a hardening parameter of $H = 16.93$. Model parameters are summarized in Table 1.

The results of structural analysis for both undamped and damped systems are presented in Figure 4. In the undamped case, the material behaves purely elastically from time step zero to time step 60. Subsequently, the trial state violates the yielding condition, leading to elastoplastic behavior. Due to plastic irreversible deformation, oscillation occurs about the -5 axis. In the damped case, a damping coefficient $c_2 = 0$ is assumed. The results exhibit purely elastic behavior until time step 62, followed by elastoplastic behavior of material. Oscillations are observed to be reduced compared to the undamped case and displacement tends towards zero due to damping.

4.1 | Numerical Verification

To validate the obtained derivatives, the results are compared with those obtained using the central FDM

$$\left(\frac{d\Phi}{d\boldsymbol{s}}\right)_{\mathrm{num}} \approx \frac{\Phi(\boldsymbol{s}+h) - \Phi(\boldsymbol{s}-h)}{2h}. \tag{11}$$

Here, the quantity of interest $\Phi(\boldsymbol{s})$ is defined as displacement, velocity, and acceleration, reducing the total variation in Equation (10) to dynamic response sensitivity matrices $\mathbf{S}_{n+1}$, $\mathbf{V}_{n+1}$, and $\mathbf{A}_{n+1}$. All control points on the top surface in the z-direction are defined as geometrical design variables, as shown in Figure 5. Perturbations ranging from $h = 10^{-8}$ to $h = 10^{2}$ are applied, and the errors between the analytical and numerical results at the last time steps are calculated using the Frobenius norm

$$\epsilon = \left\| \frac{d\Phi}{d\boldsymbol{s}} - \left(\frac{d\Phi}{d\boldsymbol{s}}\right)_{\mathrm{num}} \right\|. \tag{12}$$

These errors are then presented in Figure 6 for the undamped scenario and in Figure 7 for the damped scenario. These results confirm the accuracy of the obtained derivatives.

4.2 | Structural Response Approximation

Using sensitivity information, it is possible to approximate structural dynamic responses. To estimate displacements, the sensitivity matrix $\mathbf{S}_{n+1}$, which represents the total derivative of displacements with respect to design variables, is utilized. A design change of $\Delta\boldsymbol{s} = 0.1$ is applied. Multiplying the sensitivity matrix by the design change yields the displacement changes due to the design modification. Adding these changes to the initial displacements provides the approximated displacements

$$\mathbf{u}_{n+1}(\mathbf{s}^{\mathrm{new}}) = \mathbf{u}_{n+1}\left(\mathbf{s}^{\mathrm{init}}\right) + \mathbf{S}_{n+1}\Delta\mathbf{s}. \tag{13}$$

To verify the accuracy, the approximated results are compared with those obtained from structural analysis, showing a close match, as illustrated in Figure 8.

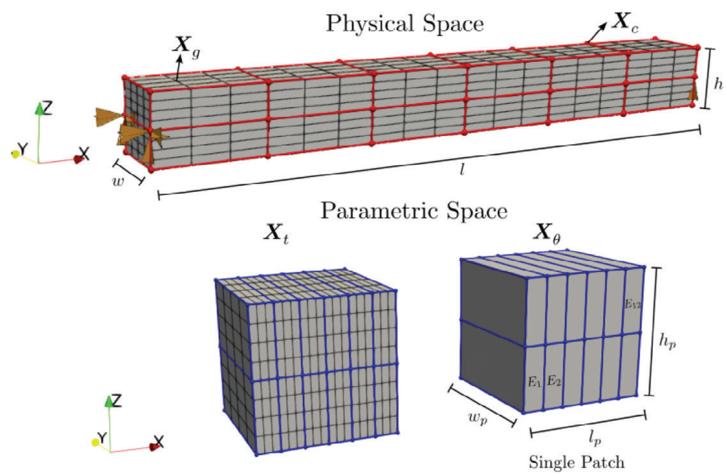

(a) Geometrical model and boundary conditions

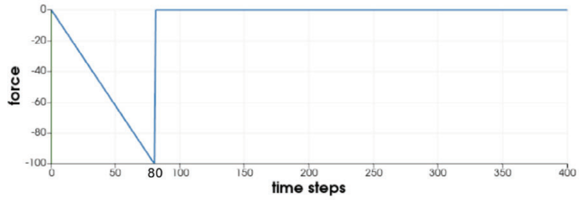

(b) Load pattern

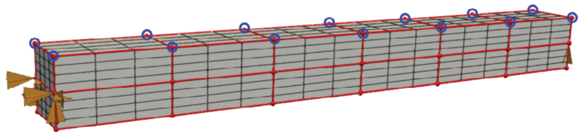

(c) Design variables

FIGURE 5 | Problem description.

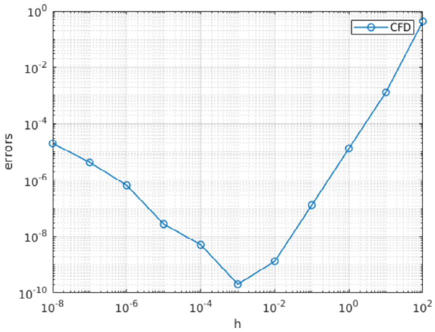

(a) $\mathbf{S}_{t=t_F}$

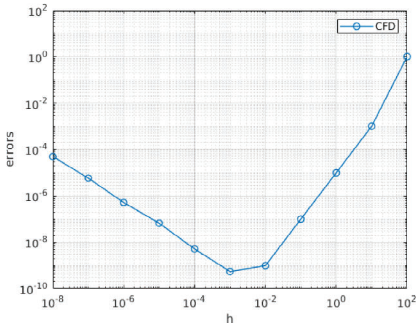

(b) $\mathbf{V}_{t=t_F}$

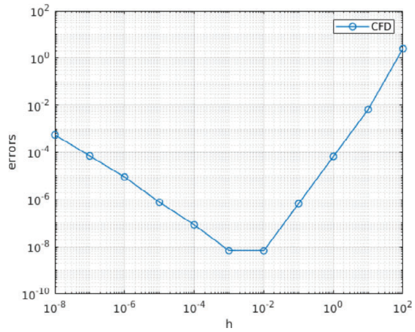

(c) $\mathbf{A}_{t=t_F}$

FIGURE 6 | Numerical verification—undamped.

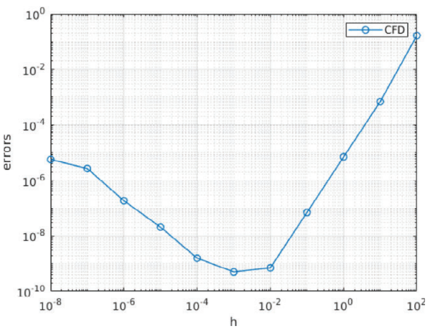

(a) $\mathbf{S}_{t=t_F}$

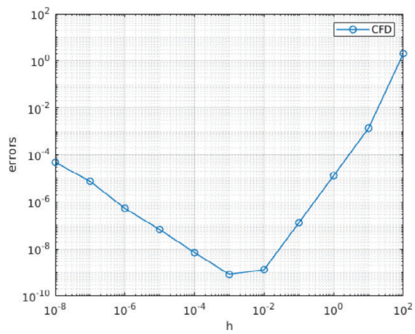

(b) $\mathbf{V}_{t=t_F}$

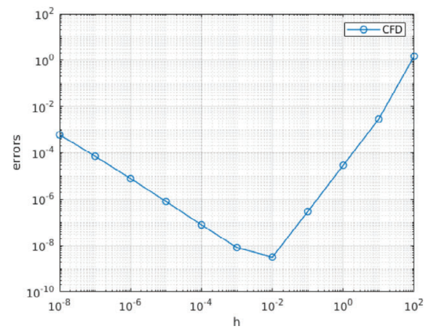

(c) $\mathbf{A}_{t=t_F}$

FIGURE 7 | Numerical verification—damped.

5 | Conclusions and Outlook

In conclusion, this work has presented a direct sensitivity analysis of dynamic structures employing history-dependent materials. IGA has been utilized for spatial discretization, while the Newmark method has been used for time discretization. Consequently, this method can be effectively applied in future research for shape optimization when dealing with a limited number of design variables. However, as the number of design variables increases, the efficiency of the DDM decreases. In such cases, the adjoint sensitivity method can be employed to obtain derivatives.

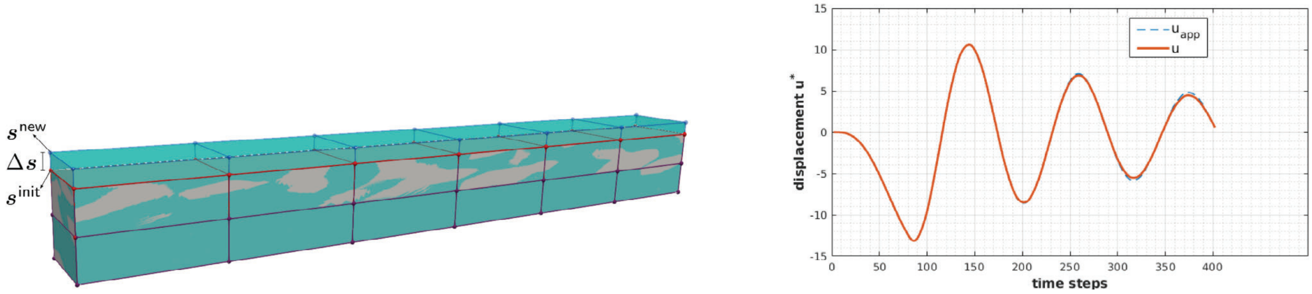

(**a**) Design change (**b**) Structural response

FIGURE 8 | Structural response approximation.

Acknowledgments

Open access funding enabled and organized by Projekt DEAL.

References

1. S. A. Ghasemi, J. Liedmann, and F.-J. Barthold, "Geometrical Design Modes of Dynamic Structures," *PAMM* 23 (2023): 1617–7061.

2. F.-J. Barthold, "Remarks on variational shape sensitivity analysis based on local coordinates," *Engineering Analysis with Boundary Elements* 32 (2008): 971–985.

3. A. Cottrell, T. Hughes, and Y. Bazilevs, *Isogeometric Analysis: Toward Integration of CAD and FEA* (Chichester, UK: Wiley, 2009).

4. L. Meyer, "Formoptimierung in der Strukturdynamik," (Diss., Universität Hannover, 1997).

5. J. Liedmann and F.-J. Barthold, "Variational Sensitivity Analysis of Elastoplastic Structures Applied to Optimal Shape of Specimens," *Structural and Multidisciplinary Optimization* 61 (2020): 2237–2251.

6. N. M. Newmark, "A Method of Computation for Structural Dynamics," *Journal of the Engineering Mechanics Division* 85, no. 3 (1959): 67–94.

7. J. C. Simo and T. Hughes, *Computational Inelasticity*, Interdisciplinary Applied Mathematics (New York: Springer, 2000).